Reconstitution Studies Using the Helical and Carboxy-Terminal Domains of Enzyme I of the Phosphoenolpyruvate:Sugar Phosphotransferase System

Peng-Peng Zhu,[‡,§] Roman H. Szczepanowski,[||] Neil J. Nosworthy,[‡,⊥] Ann Ginsburg,[||] and Alan Peterkofsky*[,‡]

Laboratory of Biochemical Genetics and Laboratory of Biochemistry, National Heart, Lung and Blood Institute, National Institutes of Health, Bethesda, Maryland 20892

Received July 21, 1999; Revised Manuscript Received September 24, 1999

ABSTRACT: Enzyme I of the bacterial phosphoenolpyruvate:sugar phosphotransferase system can be phosphorylated by PEP on an active-site histidine residue, localized to a cleft between an α-helical domain and an α/β domain on the amino terminal half of the protein. The phosphoryl group on the active-site histidine can be passed to an active-site histidine residue of HPr. It has been proposed that the major interaction between enzyme I and HPr occurs via the α-helical domain of enzyme I. The isolated recombinant α-helical domain (residues 25−145) with ∼80% α-helices as well as enzyme I deficient in that domain [EI(ΔHD)] with ∼50% α-helix content from *M. capricolum* were used to further elucidate the nature of the enzyme I−HPr complex. Isothermal titration calorimetry demonstrated that HPr binds to the α-helical domain and intact enzyme I with $K'_A = 5 \times 10^4$ and 1.4×10^5 M^{-1} at pH 7.5 and 25 °C, respectively, but not to EI(ΔHD), which contains the active-site histidine of enzyme I and can be autophosphorylated by PEP. In vitro reconstitution experiments with proteins from both *M. capricolum* and *E. coli* showed that EI(ΔHD) can donate its bound phosphoryl group to HPr in the presence of the isolated α-helical domain. Furthermore, *M. capricolum* recombinant C-terminal domain of enzyme I (EIC) was shown to reconstitute phosphotransfer activity with recombinant N-terminal domain (EIN) approximately 5% as efficiently as the HD-EI(ΔHD) pair. Recombinant EIC strongly self-associates ($K'_A \approx 10^{10}$ M^{-1}) in comparison to dimerization constants of 10^5-10^7 M^{-1} measured for EI and EI(ΔHD).

The bacterial phosphoenolpyruvate:sugar phosphotransferase system (PTS)[1] is responsible for the coupled transport across the cytoplasmic membrane together with phosphorylation of a family of sugars. The first step in the pathway involves the autophosphorylation by phosphoenolpyruvate (PEP) of an approximately 64 kDa protein (enzyme I, EI) on the N3 atom of a conserved histidine residue (His189 in *Escherichia coli*). Phosphorylated EI can, in turn, pass the phosphoryl group to the N1 atom of a conserved histidine residue (His15 in *E. coli*) of an approximately 9 kDa phosphocarrier protein, HPr. Phosphorylated HPr can transfer its phosphoryl group to a number of sugar-specific protein components, collectively known as enzymes II (*1*).

* To whom correspondence should be addressed: National Institutes of Health, Building 36, Room 4C-11, Bethesda, MD 20892. Phone: (301) 496-2408. Fax: (301) 480-0182. E-mail: alan@codon.nih.gov.

‡ Laboratory of Biochemical Genetics.

§ Present address: Molecular Plasticity Section, NINDS, NIH, Bethesda, MD 20892.

|| Laboratory of Biochemistry.

⊥ Present address: Muscle Research Unit, Department of Anatomy and Histology, Anderson Stuart Building F13, University of Sydney, NSW 2006, Australia.

[1] Abbreviations: PTS, phosphoenolpyruvate:sugar phosphotransferase system; PEP, phosphoenolpyruvate; EI, enzyme I of the PTS; HPr, histidine-containing phosphocarrier protein of the PTS; IIA^{glc}, enzyme IIA specific for glucose of the PTS; HD, the helical domain of EI (residues 25−145 in *Mycoplasma capricolum* and residues 25−143 in *Escherichia coli*; EI(ΔHD), enzyme I deleted for the helical domain; EIN, amino-terminal domain of EI (residues 1−268 of *M. capricolum*); EIC, carboxy-terminal domain of EI (residues 249-end of *M. capricolum*); PK, pyruvate kinase; PPDK, pyruvate, orthophosphate dikinase; DTT, dithiothreitol; ITC, isothermal titration calorimetry; CD, circular dichroism.

Solution and crystal structures have been elucidated for HPr and IIA^{glc} proteins from various sources (*2*−*4*). While the structure of EI has not been completely solved, that of the *E. coli* amino-terminal domain (EIN) has been determined by both X-ray (*5*) and NMR (*6*) methods. The structure of EIN ($M_r \approx 30$ kDa) is composed of two subdomains: the first contains four α-helices arranged as two hairpins to form a claw-like conformation and the second is a β-sandwich composed of a three-stranded antiparallel β-sheet and a four-stranded parallel β-sheet as well as three short α-helices. The active-site His189 is positioned in a cleft at the interface of the two subdomains.

Pyruvate, orthophosphate dikinase (PPDK) shares with EI the capability to autophosphorylate from PEP on an active-site histidine residue (*7*, *8*) as well as significant amino acid sequence homology (*9*). The PEP/pyruvate-binding domain has an eight-stranded α/β-barrel structure (*10*), which was predicted to be similar to the comparable domain of enzyme I. A sequence comparison of EIN with the phospho-histidine domain of PPDK shows little similarity except for a stretch of 12 residues in the region of the active-site histidine residue (*5*). However, a comparison of the topology of EIN and the phospho-histidine domain of PPDK suggests common elements in the two proteins; the strands of the β-sandwich of both molecules show excellent alignment and chain connectivities. A unique feature of the fold of EIN is the presence of the α-helical subdomain. Since EIN, but not PPDK, has the capability of participating in a reversible phosphotransfer with HPr, it was proposed (*5*) that the α-domain plays an important role in the HPr−EIN interaction. Models for the

10.1021/bi991680p
Published on Web 11/05/1999

Table 1: Recombinant Enzyme I Constructs[a]

construct	primers
EI(ΔHD) (*M.capricolum*)[b]	
template = pMC-EI	forward 1 = vector sequence upstream of translation start
structure = (M)(H_6)(1−24)(F)(146−end)	reverse 1 = 5′-GTATATCAAGTTTGAA**TTC**TTTTATAAC-3′
	forward 2 = 5′-CTCACATTTTAGAA*TTC***GAA**ATTCATG-3′
	reverse 2 = vector sequence downstream of translation stop
EI(ΔHD) (*E. coli*)[c]	
template = pR6	forward 1 = vector sequence upstream of translation start
structure = (M)(H_6)(1−21)(144)(K145V)(146−end)	reverse 1 = 5′-GTCAATGACAATTACTAG**TTC**TTTCAGA-3′
	forward 2 = 5′-ACATCCTGGGACTA**GTG**ATTATCGACC-3′
	reverse 2 = ptsI sequence downstream of translation stop = 5′-TATCCTTCTTGTCGACGGAAACC-3′
HD (*M.capricolum*)[d]	
template = pMC-EI	forward = 5′-AGAGCTCTTGTTATACATATG**ACC**AAACTTGATATA-3′
structure = (M)(H_6)(M)(25−145)	reverse = 5′-ATCAATAGTTGATAAGTCGACAAT*TTA***TAA**TCCTAAAATG-3′
HD (*E. coli*)[e]	
template = pR6	forward = 5′-GAAAGAAGACCATATG**GTC**ATTGACC-3′
structure = (M)(H_6)(M)(25−143)	reverse = 5′-CTCAGGTCGACAATCTT*TTA***GCC**CAGGATG-3′
EIN (*M.capricolum*)[f]	
template = pMC-EI	forward = vector sequence upstream of translation start
structure = (M)(H_6)(1−268)	reverse = 5′-CAATATTTGCGTCGACTAG*CTATTA***AAT**TTTTATCTT-3′
EIC (*M.capricolum*)[g]	
template = pMC-EI	forward = 5′-GTACAACAACATATG**GAA**TTAAAAGAGC-3′
structure = (M)(H_6)(M)(249−end)	reverse = vector sequence downstream of translation stop

[a] See Experimental Procedures for details of preparation of constructs. [b] Reverse 1 primer: underlined region = *Eco*RI recognition sequence; bold region (TTC) corresponds to codon for E24. Forward 2 primer: underlined region = *Eco*RI recognition sequence; italicized (TTC) = inserted F residue; bold region (GAA) = codon for E146. [c] Reverse 1 primer: underlined region = *Spe*I recognition sequence; bold region (TTC) = codon for E21. Forward 2 primer: underlined region = *Spe*I recognition sequence; bold region (GTG) = codon for K145 mutated to V. Reverse 2 primer: underlined region = *Sal*I recognition sequence. [d] Forward primer: underlined region = *Nde*I recognition sequence; bold region (ACC) = codon for T25. Reverse primer: underlined region = *Sal*I recognition sequence; italicized region (TTA) = stop codon; bold region (TAA) = codon for L145. [e] Forward primer: underlined region = *Nde*I recognition sequence; bold region (GTC) = codon for V25. Reverse primer: underlined region = *Sal*I recognition sequence; italicized region (TTA) = stop codon; bold region (GCC) = codon for G143. [f] Reverse primer: underlined region = *Sal*I recognition sequence; italicized region (CTATTA) = tandem stop codons; bold region (AAT) = codon for I268. [g] Forward primer: underlined region = *Nde*I recognition sequence; bold region (GAA) = codon for E249.

HPr−EIN transition state complex (*11*) and the solution structure of the HPr−EIN complex (*12*) support the idea that the major interactions of HPr with EI involve interactions with the α-domain.

In our continuing studies of PTS proteins in *M. capricolum* (*3*, *4*, *13*−*16*), we experimentally tested the model that the α-helical domain of EI is necessary for interaction with HPr. Evaluation of the binding and phosphotransfer capabilities of isolated subdomains from *M. capricolum* established the requirement of the α-helical region for binding to HPr.

Enzyme I undergoes a monomer−dimer association, but EIN is a monomer (*17*, *18*). It has therefore been postulated that the carboxyl-terminal domain of EI (EIC) is the determinant of the association (*18*). The availability of the cloned regions of EI deficient either in the α-helical domain [EI(ΔHD)] or in the amino-terminal domain (EIC) provided the possibility to explore the requirement of these segments of the protein for the dimerization reaction and reconstitution of PTS activity in both *E. coli* and *M. capricolum*.

EXPERIMENTAL PROCEDURES

Materials. Oligonucleotides were synthesized using a model 394 DNA/RNA synthesizer (Applied Biosystems). Restriction endonucleases and T4 DNA ligase were purchased from New England Biolabs and Boehringer Mannheim. Tryptophan was purchased from Bethesda Research Laboratories. [γ^{32}P]ATP was purchased from NEN. Essentially homogeneous preparations of *E. coli* EI (*19*), *M. capricolum* EI (*20*), *E. coli* HPr (*19*), His-tagged *M. capricolum* HPr (*16*), *E. coli* IIA^{glc} (*19*), and *M. capricolum* IIA^{glc} (*16*) were purified as previously described.

DNA Methods. *Construction of Expression Vectors*. *(A)* Vector encoding EI(ΔHD) from *M. capricolum*. pMC-EI (*20*), a vector encoding EI from *M. capricolum*, was used as a template for two PCR reactions to amplify DNA encoding residues 1−24 of EI (reaction 1) and residues 146 through the end of the EI sequence (reaction 2, see Table 1). PCR products 1 and 2 were digested with *Eco*RI and ligated. The purified ligation product was then digested with *Nde*I and *Sal*I and then ligated to the appropriately digested vector pRE-His-Tag (*16*), resulting in a construct encoding a His-tagged form of EI missing the α-helical domain. As a consequence of the fusion methodology, a phenylalanine residue was inserted between the end of the first β-sheet and the remainder of the protein (see Table 1).

(B) Vector encoding EI(ΔHD) from *E. coli*. pR6 (19), a vector encoding EI from *E. coli*, was used as a template for two PCR reactions to amplify DNA encoding residues 1−21 of EI (reaction 1) and residues 144 through the end of the EI sequence (reaction 2, see Table 1). PCR products 1 and 2 were digested with *Spe*I and ligated. The purified ligation product was then digested with *Nde*I and *Sal*I and then ligated to the *Nde*I−*Sal*I fragment of the vector pRE-His-Tag, resulting in a construct encoding a His-tagged form of EI missing the α-helical domain. The recombinant DNA methodology used resulted in a fusion in which K145 of EI was mutated to V (see Table 1).

(C) Vector encoding HD from *M. capricolum*. pMC-EI was used as a template for a PCR reaction to amplify the

region encoding residues 25−145 of EI. The PCR product was digested with *Nde*I and *Sal*I and ligated to pRE-His-Tag, which had been digested with the same enzymes, resulting in a construct encoding a His-tagged form of the α-helical domain of EI.

(D) Vector encoding HD from *E. coli*. pR6 was used as a template for a PCR reaction to amplify the region encoding residues 25−143 of EI (see Table 1). The PCR product was digested with *Nde*I and *Sal*I and ligated to pRE-His-Tag, which had been digested with the same enzymes, resulting in a construct encoding a His-tagged form of the α-helical domain of EI.

(E) Vector encoding EIN from *M. capricolum*. pMC-EI was used as a template for a PCR reaction to amplify the region encoding residues 1−268 of EI (see Table 1). The PCR product was digested with *Nde*I and *Sal*I and ligated to pRE-His-Tag, which had been digested with the same enzymes, resulting in a construct encoding a His-tagged form of the N-terminal region of EI.

(F) Vector encoding EIC from *M. capricolum*. pMC-EI was used as a template for a PCR reaction to amplify the region encoding residues 249 to the end of the EI sequence (see Table 1). The PCR product was digested with *Nde*I and *Sal*I and ligated to pRE-His-Tag, which had been digested with the same enzymes, resulting in a construct encoding a His-tagged form of the C-terminal region of EI.

(G) Vector encoding His-tagged EI from *M. capricolum*. pMC-EI was digested with *Nde*I and *Sal*I and the fragment encoding EI was ligated to similarly digested pRE-His-Tag, resulting in a construct encoding a His-tagged form of EI.

All the constructs were verified by DNA sequencing by the dideoxy method of Sanger et al. (*21*) using an Applied Biosystems automated sequencer. Plasmids were introduced into a *pts* deletion derivative of *E. coli* GI698 by electroporation as described previously (*17*).

Expression and Purification of Recombinant Proteins. Transformants in GI698Δpts were grown as described (*22*) to $A_{600} \approx 0.6$, and then tryptophan was added to induce the expression of the proteins. Induction was continued overnight. The cells were then harvested and disrupted and the supernatant solutions after centrifugation at 35000*g* were purified as previously described (*16*) using Ni-NTA-agarose (Qiagen, 3 mL bed volume). The unadsorbed proteins were washed off the column with 50 mL of buffer (50 mM Tris, pH 8.0, 300 mM NaCl), and the protein of interest was eluted from the column with 12 mL of the same buffer containing 0.1 M imidazole. The eluates were concentrated and dialyzed against 25 mM Tris, pH 7.5, and then further purified by FPLC chromatography on a MonoQ HR 10/10 column (Pharmacia), using the pH 7.5 Tris buffer and a gradient from 0 to 0.4 M NaCl. Fractions enriched in the protein of interest, as judged by SDS−PAGE, were pooled and concentrated. All the purified proteins were approximately 95% pure. Protein concentrations for HPr were determined by the method of Waddell (*23*). The concentrations of EI fragments were determined by absorbance at 280 nm, 1 cm: for EI and EI(ΔHD) = 0.400 cm^2/mg; for EIC = 0.475 cm^2/mg.

Isothermal Titration Calorimetry. The titrations were performed in MCS−ITC and VP−ITC isothermal titration calorimeters (MicroCal, Northampton, MA). All samples were dialyzed overnight in 10 mM K·PO_4, pH 7.5, containing 100 mM KCl and 1 mM EDTA (buffer A). HPr concentration in the syringe was approximately 350 μM and that of the proteins in the cell (∼ 1.4 mL) was about 30 μM. Twelve or eighteen injections (15 or 20 μL) were used in each experiment at a temperature of 25.0 °C such that the final molar ratio of HPr to the other protein was 2.5−3:1. For further details, see the legend to Table 2. Data analysis used ITC Origin software (MicroCal).

Analytical Ultracentrifugation. A Beckman Optima model XL-A ultracentrifuge (Beckman Instruments, Inc.) equipped with a four-place titanium rotor was used at either 4.0 or 20.0 °C. Buffer densities were determined at 20.00 ± 0.01 °C with an Anton Paar model DMA-58 densitometer. Prior to ultracentrifugation, EI fragments were dialyzed overnight against 1000× volumes of buffer containing 20 mM K·PO_4, 100 mM KCl, and 2 mM 2-mercaptoethanol, pH 7.5 (buffer B) (density at 20.0 °C = 1.0057 g/mL). Partial specific volumes of 0.728 mL/g for wild-type EI without a His tag and 0.726 and 0.724 mL/g for EI(ΔHD) and EIC with Met-$(His)_6$ tags, respectively, were calculated from amino acid compositions and the values of Zamyatnin (*24*). Sedimentation equilibrium experiments utilized a carbon-filled, six-channel centerpiece in a 12 mm cell. Increasing concentrations of protein (0.100 mL/channel) having ∼0.11, 0.24, and 0.35 absorbances at 280 nm (1.2 cm light path) vs 0.110 mL dialyzate buffer in reference channels were used. Global analysis for sedimentation equilibrium data using a reversible, associating monomer−dimer model was applied to data sets obtained from radial scans at 0.001 cm (step mode) at 280 nm for three concentrations of protein after 28, 32, 36, 40, and 44 h at the indicated speed. Baseline corrections were zero in all cases. Estimates of the fraction of aggregated protein in the EIC sample were obtained from a nonequilibrium model. These analyses as well as global fitting to various reversibly associating models for data obtained at different concentrations and/or speed were performed with software kindly provided by Allen P. Minton (NIDDK, NIH), which can be downloaded from the following World Wide Web site: http://www.bbri.org/RASMB/rasmb.html.

Circular Dichroism. CD measurements were performed with a Jasco J-710 spectrometer as previously described using a 0.02 cm water-jacketed cylindrical cell at 20 °C (*16*). Samples containing enzyme I (1.17 mg/mL; average residue weight = 113.0), HD (0.95 mg/mL; average residue weight = 116.1), and EI(ΔHD) (1.04 mg/mL; average residue weight = 112.7) were from the ITC studies in buffer A. EIC (1.10 mg/mL; average residue weight = 114.2) was from the ultracentrifugation studies in buffer B. Secondary structural components were calculated by the method of Yang et al. (*25*) using software supplied by Jasco, Inc.

Phosphorylation of IIA^{glc}. Phosphotransfer from [^{32}P]PEP to HPr and IIA^{glc} was measured in a reaction mixture (10 μL) containing 100 mM Tris·HCl, pH 7.5, 2 mM $MgCl_2$, 1 mM EDTA, 0.5 mM DTT, 1 mM pyruvic acid, 0.01 unit pyruvate kinase (Boehringer-Mannheim), 0.2 mM [^{32}P]ATP (∼220 cpm/pmol), and 1 μg each of the specified HPr, EI derivative and IIA^{glc}. The combination of pyruvate kinase, pyruvic acid, and [^{32}P]ATP was used to generate [^{32}P]PEP in vitro. Incubation was at room temperature for 10 min. The mixture was then electrophoresed on an SDS−polyacrylamide gel (4−20% Tris·glycine, Novex). The gel was

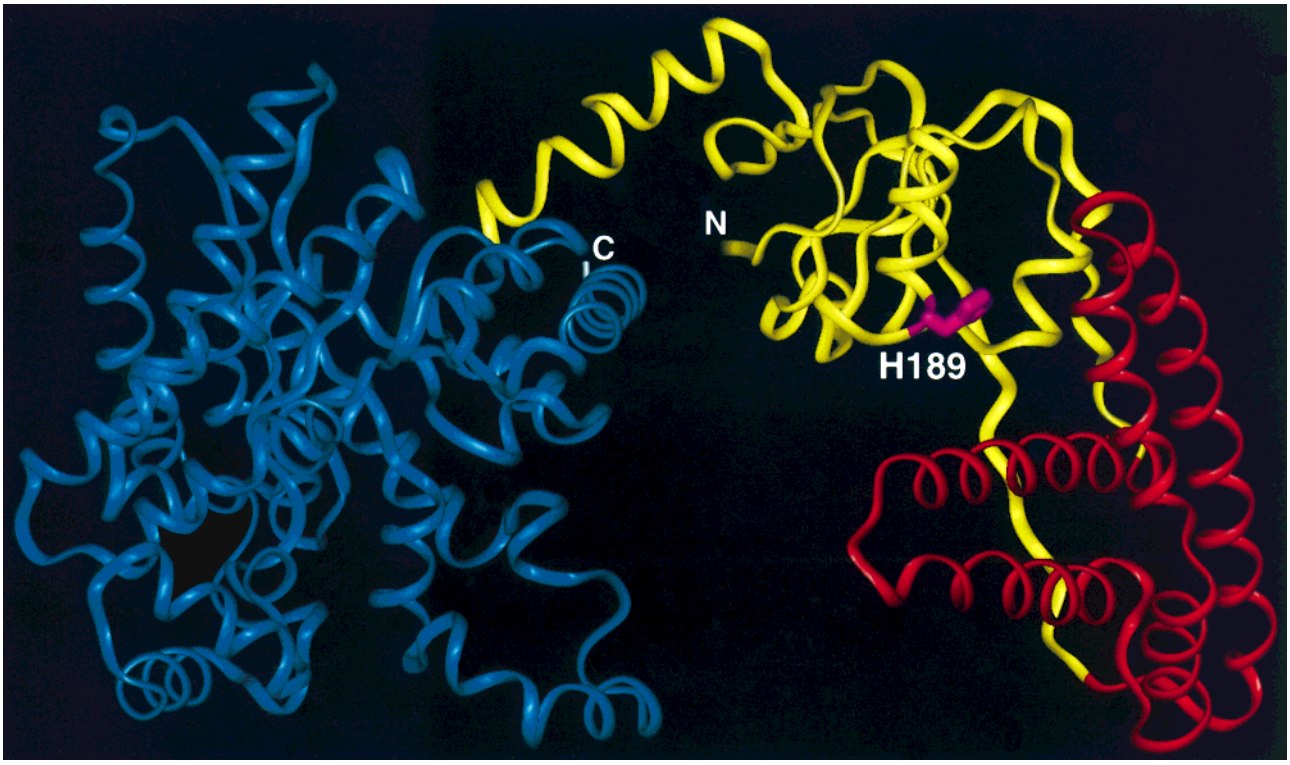

FIGURE 1: Model of enzyme I structure. The cartoon shows a working model for the structure of enzyme I. It was constructed by molecular modeling, using Insight II (Molecular Simulations, Inc., San Diego, CA), to create a fusion of EIN (using 1ZYM of the Brookhaven Protein Data Base, shown in red and yellow, see text) to the PEP/pyruvate domain of PPDK (using 1DIK of the Brookhaven Protein Data Base, residues 534−874, shown in blue), The side chain of the active-site His189 is shown in magenta. The red α-helical domain corresponds to the presumptive HPr binding region. The yellow domain contains the active-site. The blue domain corresponds to the presumptive PEP-binding region.

stained with Coommassie Blue and dried. Autoradiography was carried out using Kodak XAR film.

In Vitro Sugar Phosphorylation. Assays for PTS activity were carried out in vitro according to Zhu et al. (*14*) using cell-free extract from TP2811 (*26*) as a source of membrane-bound enzyme $IIBC^{glc}$. Reaction mixtures (50 μL) contained 0.1 mM [^{14}C]methyl α-glucoside (5600 cpm/nmol); 2 mM PEP; 100 mM Tris·HCl, pH 7.4; 2 mM $MgCl_2$; 1 mM DTT; 10 μL of TP2811 cell-free extract described above; 5 μg of HPr; 1 μg of Enzyme IIA^{glc}; and the indicated amounts of EI derivatives [as nanograms of full-length EI or milligrams of HD or EI(ΔHD)]. Tests of the activity conferred by EIN or EIC used 5 μg of those proteins. Reaction mixtures were incubated at 37 °C for 20 min before and then 10 min after the addition of radioactive sugar substrate and PEP. The reaction rate was limited by the amount of EI derivative added to incubation mixtures. After incubation, the reaction mixtures were processed for measurement of radiolabeled sugar−phosphate production as described (*27*).

RESULTS

Construction of EI Domains. A cartoon representation of a model of the structure of EI is shown in Figure 1. The structure of the amino-terminal domain (EIN), represented as the red (presumptive HPr-binding domain) and yellow (active-site domain) segments of Figure 1, of *E. coli* EI has been solved (*5*, *6*), but that of the carboxyl-terminal domain has not. There is a high degree of homology between the EI C-terminal domain and the PEP/pyruvate domain of PPDK, shown as the blue (presumptive PEP-binding domain) segment of Figure 1. The availability of the two structures (*5*, *6*, *10*) allowed us to create a composite working structure by molecular modeling. Thus, EIN (*E. coli*) was fused to the PEP/pyruvate domain of PPDK (*C. symbiosis*). This is expected to correspond to some approximation of the actual structure of EI, although the precise relationship of the EIN portion to the remainder of the molecule is not defined.

A comparison of the fold of EIN to the phosphohistidine domain of PPDK made clear a substantial similarity in the two structures. However, since the α-helical domain of EIN is unique to that molecule, it was suggested that the α-helical domain is specialized for interaction with HPr (*5*). One of the major objectives of this study was to evaluate the importance of the α-helical domain for its capability to associate with HPr. Consequently, modified forms of EI deficient in the α-helical domain as well as the isolated α-helical domain were prepared from both *E. coli* and *M. capricolum* (see Table 1).

An alignment of the amino terminal regions of EI from *E. coli* and *M. capricolum* is shown in Figure 2. The shaded regions correspond to the α-helical domains (helices 1−4). As described in the Experimental Procedures and Table 1, recombinant DNA constructs were made that were capable of high-level expression of the isolated α-helical domains (HD) as well as the protein deficient in the helical domain [EI(ΔHD)] from both *E. coli* and *M. capricolum*. The proteins were expressed and purified (see Experimental Procedures), resulting in products that were at least 95% pure (see Figure 3).

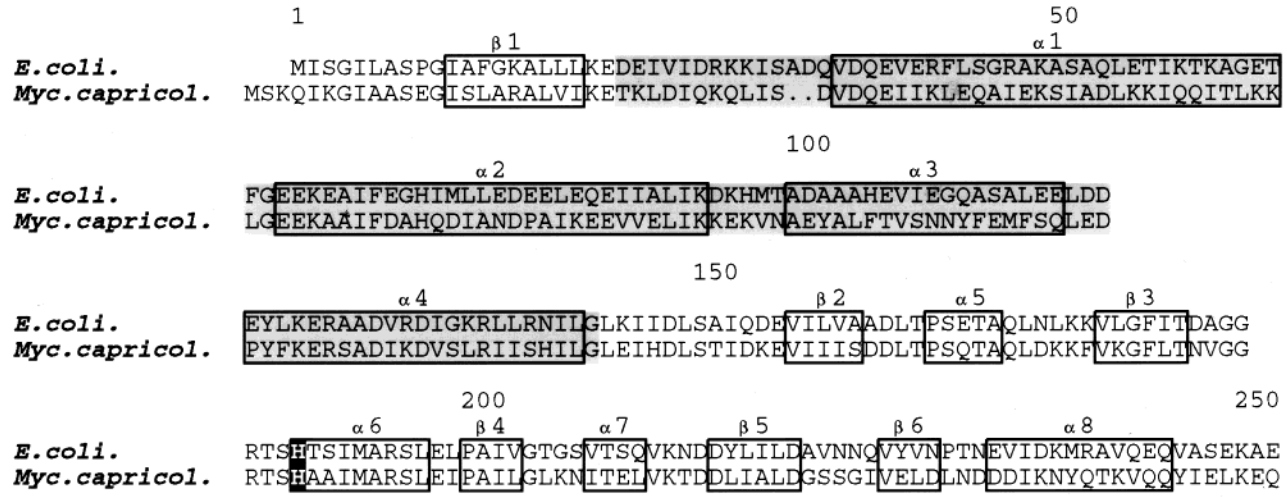

FIGURE 2: Multiple sequence alignment of the N-terminal regions of enzyme I proteins from *E. coli* and *M. capricolum*. The alignments were constructed and highlighted using the DNADRAW program. The shaded region corresponds to the α-helical domain and the boxed regions to each of the α-helices and *β*-strands. The active-site histidine residue is shown in reverse shading. Genbank Accession numbers for the sequences are *E. coli*, M10425; *M. capricolum*, U15110.

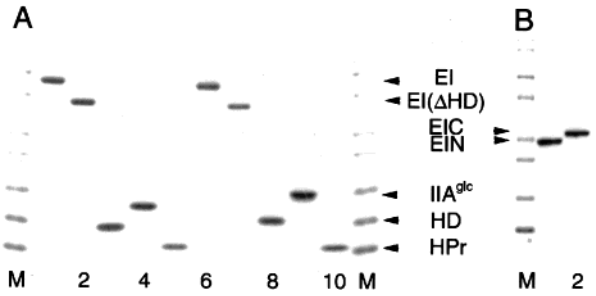

FIGURE 3: SDS−PAGE of purified PTS proteins. SDS−PAGE of the purified proteins (approximately 1 μg) was performed using 4 to 20% gradient gels (NOVEX, San Diego). The gels were stained with Coomassie blue. M indicates Mark 12 protein molecular weight standards (NOVEX). (A) Lane numbers correspond to the following proteins: 1 and 6, EI; 2 and 7, EI(ΔHD); 3 and 8, HD; 4 and 9, IIA^{glc}; 5 and 10, HPr. Lanes 1−5 correspond to *M. capricolum* proteins and lanes 6−10 are *E. coli* proteins. (B) Lane 1, EIN (*M. capricolum*); lane 2, EIC (*M. capricolum*).

Interaction of HPr with EI Domains. The idea that the region of EI associated with the binding of HPr is the α-helical domain was tested directly by isothermal titration calorimetry. A concentrated solution of *M. capricolum* HPr was loaded into the injection syringe and added in increments up to a molar ratio of approximately 3 to various *M. capricolum* EI derivatives. (Figure 4). A control injection of HPr into the buffer (Figure 4A and Experimental Procedures) elicited no significant heat. As expected, HPr binding to EI was detected (Figure 4B). The apparent association constant (K'_A) determined in three different titrations was (1.3−1.6) × 10^5 M^{-1} (see Table 2), which was similar to K'_A values previously reported (*28*) for the interaction of *E. coli* EI (1.1 × 10^5 M^{-1}) or EIN (1.4 × 10^5 M^{-1}) with *E. coli* HPr. The measured stoichiometry of binding of HPr to EI was 0.9, consistent with a 1:1/HPr:EI complex formation, taking into account the error in determining the HPr concentration (see Table 2). The heat of binding of *M. capricolum* HPr to *M. capricolum* EI (ΔH = 4300−4800 cal/mol) is lower than that previously reported for the interaction of *E. coli* HPr with *E. coli* EI (6200 cal/mol) or *E. coli* EIN (8760 cal/mol) (*28*) using the same pH 7.5 phosphate buffer at 25 °C as in our experiments. The enthalpic difference for the HPr:EI interaction with proteins from *M. capricolum* and *E. coli* is probably due to structural differences in the proteins from the two sources.

In contrast to the clear demonstration of an HPr-EI interaction (Figure 4B), there is no detectable interaction of HPr with EI(ΔHD) (Figure 4C). These data are consistent with the previous suggestion (*5*, *12*) that the α-helical domain of EI is essential for the interaction with HPr.

The notion that the isolated α-helical domain, by itself, is able to interact with HPr was tested (Figure 4D). The results clearly demonstrated that HD itself binds HPr. The K'_A for the association was, however, about 3-fold lower than that for EI−HPr (~0.5 × 10^5 M^{-1} vs 1.4 × 10^5 M^{-1} at pH 7.5, 25 °C; see Table 2) and the heat of reaction was significantly lower than that observed for full-length EI. The stoichiometry was 1.4−1.7, suggesting that more than 1 equivalent of HPr might bind to isolated HD.

A final titration in which HPr was injected into an equimolar mixture of HD and EI(ΔHD) is shown in Figure 4E. The results were essentially the same as for the HD alone (Figure 4D). This suggests that HD does not associate with EI(ΔHD). Also, a titration experiment (data not shown) failed to detect an association between HD and EI(ΔHD).

Since the association of HD with HPr was found to be considerably weaker (~3-fold, see above) than with EI, the possibility was considered that isolated HD unwinds, resulting in loss of capability to interact with HPr. Consequently, some of the *M. capricolum* proteins used in this study were examined by CD (Figure 5). The far UV−CD spectra of EI, EI(ΔHD), and EIC were essentially the same, and the calculated helix content was from 50 to 55%. In contrast, the isolated HD gave a different CD spectrum and the helix content was calculated to be 80%. Therefore, the weaker association of HPr with HD cannot be explained by loss of helices, although it cannot be excluded that the orientation of the two helical hairpins with respect to one another may be different in HD compared to EI. In fact, the stoichiometry of binding HPr (>1) indicates that additional sites for HPr interaction with HD exist.

Domain Requirements for EI Dimerization. Intact EI is subject to a monomer−dimer association (*29*). The avail-

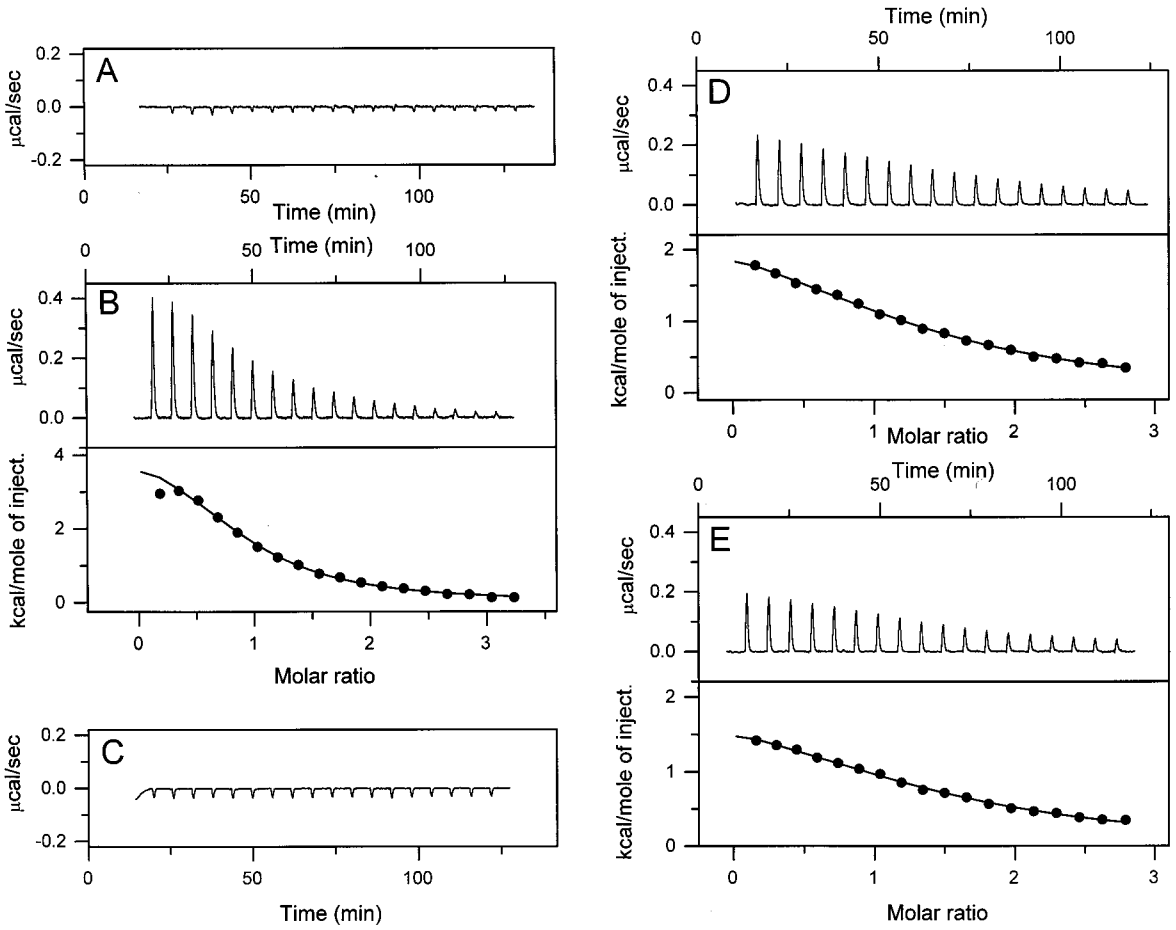

FIGURE 4: Titration of PTS proteins with HPr using VP−ITC. The binding of *M. capricolum* HPr to various *M. capricolum* EI fragments was studied by isothermal titration calorimetry using the VP−ITC at 25.0 °C (see Experimental Procedures and Table 2). (A) Titration of HPr into buffer; (B) titration of HPr into EI; (C) titration of HPr into EI(ΔHD); (D) titration of HPr into HD; (E) titration of HPr into a mixture of HD and EI(ΔHD).

Table 2: Thermodynamic Parameters for Interaction of HPr with EI and EI Fragments at pH 7.5 and 25 °C[a]

proteins	K'_A (10^5 M^{-1})	ΔH (cal/mol)	n (mol/mol)[b]
EI[c]	1.4	4700	0.9
EI[d]	1.3	4800	0.9
EI[e]	1.6	4300	0.8
HD[c]	0.50	2800	1.4
HD[e]	0.51	3400	1.7
HD + EI(ΔHD)[c]	0.47	2200	1.5
HD + EI(ΔHD)[e]	0.31	4700	1.3

[a] Isothermal titration calorimetry experiments with *M. capricolum* proteins were performed as described in Experimental Procedures. Proteins were dialyzed against 10 mM K·PO_4, 100 mM KCl, and 1 mM EDTA, pH 7.5. Errors in the fits of titration data for K'_A, ΔH, and n were $\pm 9 \times 10^3$ M^{-1}, ±200 cal/mol, and ±0.1, respectively. [b] The major source of error in this calculation involves the determination of the concentration of HPr. For this reason, the concentration of HPr was determined in triplicate. [c] Eighteen injections at 15 µL. [d] Twelve injections at 20 µL in the VP−ITC. [e] Twelve injections at 20 µL in the MicroCal MCS.

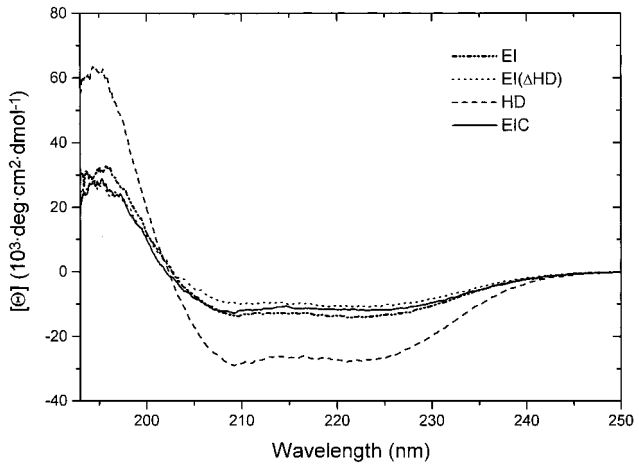

FIGURE 5: Far UV−CD spectra for *M. capricolum* enzyme I and fragments. CD measurements were performed as described in Experimental Procedures. The spectra shown are EI (—••—); EI(ΔHD) (•••); HD (- - -), and EIC (—).

ability of the collection of *M. capricolum* EI derivatives deficient in certain domains made it possible to evaluate the dependence on different parts of the structure for dimer formation by sedimentation equilibrium studies (see Table 3). Previous data on *E. coli* EI indicated that dimer formation was decreased at lower temperatures (*30*). In the case of *M. capricolum* EI, there is a monomer−dimer association, but it is not significantly influenced by temperature (*16*). Dimerization constants (log K'_A = 5.1 at 20 °C and 5.6 at 4 °C) for *M. capricolum* were reported previously (*16*). EI(ΔHD) also shows a monomer−dimer association, which is not significantly affected by temperature (log K'_A = 6.5 at 20 °C and 6.9 at 4 °C). The data indicate that removal of HD from EI to give EI(ΔHD) actually promotes dimerization with an approximately 10-fold increase in the subunit

Table 3: Sedimentation Equilibrium Studies on *M. Capricolum* Enzyme I and Fragments (pH 7.5)[a]

protein	monomer M_r[b]	T (°C)	speed (rpm)	dimerization constant[c] log K'_A (M monomer)$^{-1}$
enzyme I[d]	64 602	4.0	11 000	5.6[d]
		20.0	11 000	5.1[d]
enzyme I (ΔHD)	51 831	4.0	10 000	6.9 ± 0.3
		20.0	10 000	6.5 ± 0.1
enzyme I C-terminal domain	38 027	4.0	12 000; 16 000	10 ± 1[e]

[a] See Experimental Procedures for ultracentrifugation conditions and data analysis. [b] Monomer molecular weights were calculated from amino acid compositions; EI(ΔHD) and EIC contained the His tag: Met$(His)_6$. [c] Monomer M_r values were constrained during global, nonlinear least-squares fitting procedures. In all cases, the fitted concentration gradients ($\delta A/\delta R$) gave random distributions of residuals which were $\leq \pm 0.01$ absorbance units. Standard errrors for log K'_A values were calculated from four to five different data sets. [d] This set of data was from ref *16* and is presented for purposes of comparison. The EI used in this study was not His-tagged. [e] The EIC protein sample contained ~1% of a nonequilibrium aggregate.

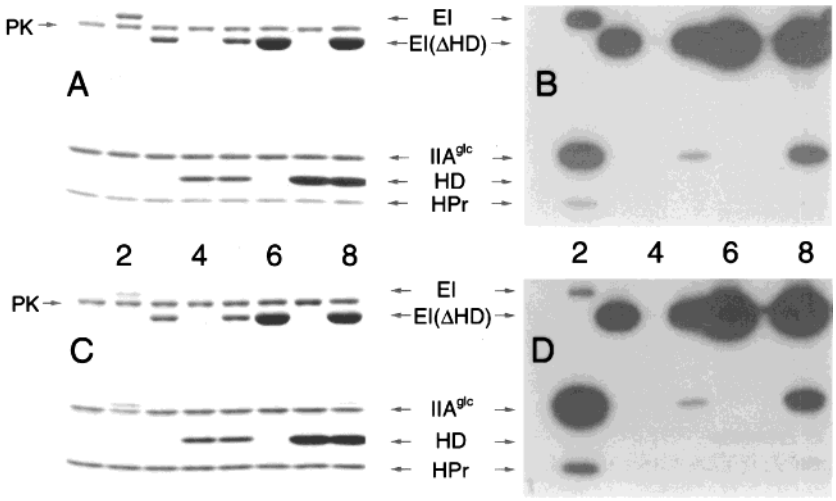

FIGURE 6: Phosphotransfer studies with PTS proteins. [^{32}P]PEP was generated during reactions from [γ-^{32}P]ATP and pyruvate kinase. Phosphotransfer reactions were performed as described in Experimental Procedures. Lane 1, control, no added enzyme I fragment; lane 2, EI; lane 3, EI(ΔHD); lane 4, HD; lane 5, HD + EI(ΔHD); lane 6, EI(ΔHD) (4 μg); lane 7, HD (4 μg); lane 8, EI(ΔHD) + HD, both at 4 μg. Panels A and B show the data with proteins from *M. capricolum* and panels C and D show the data with proteins from *E. coli*. The *E. coli* EI was not His-tagged, while all the other EI derivatives were His-tagged.

association constant (see Table 3). Since it has been observed that EIN is monomeric (*17*, *18*), it was suggested that the capacity for dimerization of EI resides in EIC (*18*). The availability of purified EIC from *M. capricolum* allowed us to determine if the isolated EIC domain dimerizes (see Table 3). A sedimentation equilibrium experiment at 4 °C showed that at 6 μM subunit concentration, for example, essentially all of EIC is dimeric with <1% monomer and ~1% of an aggregated species present (Table 3). The results indicate that EIC self-associates with a higher affinity constant than EI or EI(ΔHD). Consequently, the EIN portion of EI appears to diminish the potential of EI to dimerize.

*Reconstitution of Phosphotransfer Activity.*The capability of EI(ΔHD) to become phosphorylated by PEP and participate in phosphoryl transfer to HPr in the presence of HD was tested in vitro using purified proteins (see Figures 3 and 6). The reaction conditions were set up such that the molar concentration of IIA^{glc} was approximately 5-fold higher than that of EI. Consequently, P−IIA^{glc} accumulated and was in equilibrium with HPr. Experiments were carried out with proteins from both *M. capricolum* (Figure 6, panels A and B) and *E. coli* (Figure 6, panels C and D).

As expected, EI is able to both accept and transfer a phosphoryl group derived from PEP (Figure 6, lane 2). Consequently, label appears in EI, HPr, and IIA^{glc} of Figure 6, panels B and D.

EI(ΔHD) is autophosphorylated by PEP but is incapable of phosphoryl transfer to HPr (lane 3). As a result, only the EI(ΔHD) protein, but not HPr or IIA^{glc}, becomes radioactive (Figure 6, lane 3 of panels B and D). These results are consistent with the findings from isothermal titration calorimetry which showed no association of EI(ΔHD) with HPr (panel C of Figure 4).

HD is completely inactive as a phosphoryl acceptor since it does not contain the active-site His residue; consequently, HD by itself does not promote phosphoryl transfer (Figure 6, lane 4 of panels B and D).

A series of tests designed to recognize a reconstitution of phosphotransfer activity by mixtures of HD and EI(ΔHD) were performed (lanes 5−8). When reaction mixtures contained 1 μg of each protein, only a trace of IIA^{glc} became labeled (Figure 6, lane 5 of panels B and D). However, increasing the concentration of the protein fragments 4-fold resulted in a significant reconstitution of phosphotransfer activity (Figure 6, lane 8 of panels B and D). However, the extent of labeling of IIA^{glc} was substantially less than that observed with EI (lane 2), suggesting only a weak association between HD and EI(ΔHD).

In vitro phosphorylation of methyl α-glucoside from [^{32}P]-PEP, under conditions where EI is limiting, provided a basis for a quantitative comparison of the phosphotransfer activity of EI and the mixture of HD and EI(ΔHD) (Figure 7). The

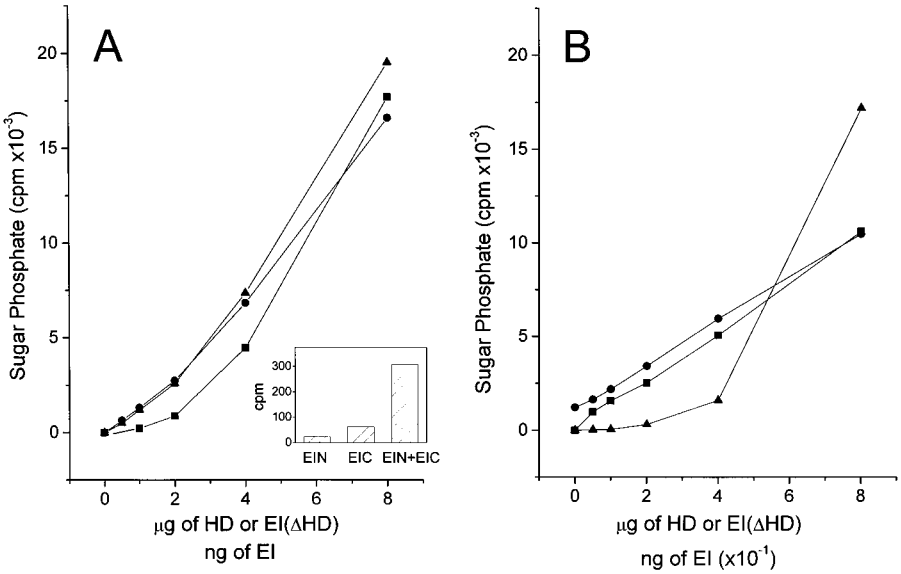

FIGURE 7: In vitro sugar phosphorylation. Assays for PTS activity were performed in vitro (see Experimental Procedures) using cell-free extract from *E. coli* TP2811 as a source of membrane-bound enzyme IIBC^{glc}. The activity with limiting amounts of EI (▲) is compared to that with saturating amounts of HD (5 μg) titrated with various amounts of EI(ΔHD) (●) or saturating amounts of EI(ΔHD) (5 μg) titrated with various amounts of HD (■). Panel A shows the data using purified proteins from *M. capricolum* while panel B shows the data using purified proteins from *E. coli* (see Figure 3). The *E. coli* EI was not His-tagged, while all the other EI derivatives were His-tagged. Inset: sugar phosphorylation activity using EIN, EIC, or a mixture of EIN and EIC as a source of the EI component.

experiments were carried out with purified proteins from both *M. capricolum* (Figure 7A) and *E. coli* (Figure 7B). An extract of a Δ*pts* strain of *E. coli* was used as a source of membrane-associated IIBC^{glc} (*26*) for both studies.

For EI (triangles), a concentration range from 2 to 8 ng for *M. capricolum* (panel A) and 40−80 ng for *E. coli* (panel B) produced an approximately linear response in the sugar phosphorylation assay. In another set of experiments, HD was kept constant at 5 μg/assay, and the concentration of EI(ΔHD) was varied up to 8 μg/assay (circles). Similarly, a series of tests was carried out in which EI(ΔHD) was maintained at 5 μg/assay and the concentration of HD was varied up to 5 μg/assay (squares). The results show that phosphotransfer to methyl α-glucoside is reconstituted but that intact *M. capricolum* EI is approximately 1000 times as effective and intact *E. coli* EI is approximately 100 times[2] as effective as the mixture of the two fragments. Either fragment alone is essentially inactive.

The inset to Figure 7A shows data for reconstitution of PTS activity by a mixture of EIN and EIC from *M. capricolum*, using 5 μg of each component per assay. While neither EIN nor EIC alone catalyzed sugar phosphorylation, the mixture of the two proteins exhibited significant activity. However, the activity seen in the EIN−EIC reconstitution was approximately 5% of that observed using similar concentrations of HD and EI(ΔHD).

DISCUSSION

EI is the first protein in the phosphotransfer cascade of the PTS. It is required to not only interact with and be autophosphorylated by PEP but also to interact with and participate in phosphotransfer to HPr. The protein is of relatively high molecular mass (~64 kDa) and has multiple domains. Another feature of the enzyme involved in controlling its activity is its capability to associate to form dimers (*1*, *29*).

Proteolysis experiments have established the overall structure of EI to be composed of a relatively compact amino-terminal half linked to a proteolytically sensitive carboxyl-terminal half (*31*, *32*). Up to this time, it has not been possible to deduce the 3-D structure of EI. However, the compact amino-terminal half, EIN, has been amenable to such analysis. Solution and X-ray structures of EIN (*5*, *6*) have demonstrated the presence of two subdomains, an α/*β*-domain and an α-domain. The α/*β*-domain has a similar fold to that of the phospho-histidine domain of PPDK (*10*), suggesting that this region plays a role in the autophosphorylation reaction. Since the presence of the α-domain and the capability to interact with HPr are unique to EIN, it was proposed that the α-domain is specialized for the interaction with and phosphotransfer to HPr.

The structure of PPDK (*10*) showed a region associated with dimer formation that was homologous to EIC. This is consistent with our findings that *M. capricolum* EIC dimerizes. The analysis of the variety of constructs described here by ultracentrifugation has permitted us to establish that EIC dimerizes more effectively than EI. It may be that a more physiologically meaningful distribution of monomers and dimers is effected by the complete structure of EI since PTS activity of the reconstituted mixture of EIN and EIC is considerably less than that of intact EI (see Figure 7). It has been suggested that modulation of the monomer−dimer ratio in EI may be a regulatory mechanism (*29*).

The availability of the structure of EIN together with sequence similarity of EIC to the PEP/pyruvate domain of PPDK, which is an α/*β* barrel (*10*), has allowed us to formulate a tentative working model for the structure of EI,

[2] The preparation of *E. coli* EI used showed considerable aggregation. We estimate that approximately 10% was not aggregated [compare Figure 5, lane 2 of panels A (*M. capricolum*) and C (*E. coli*)]. Consequently, *E. coli* EI is probably also 1000 times as effective as the mixture of the two fragments.

shown in Figure 1. Until a 3-D structure of EI is available, however, the details of the spatial relationship of EIN to EIC are uncertain.

Both molecular modeling (*11*) as well as NMR analysis of the HPr−EIN complex (*12*) have provided strong evidence for the interaction of HPr with EIN primarily by an all-helical interface involving the helical domain of EIN and helices 1 and 2 of HPr (*12*). The present work has extended and confirmed these studies by examining the capability of isolated regions of EI to function independently in the interaction with HPr. In this regard, a recombinant DNA approach was used to generate purified preparations of HD and EI(ΔHD) for activity testing.

ITC experiments clearly established that HD binds HPr and, conversely, elimination of HD from the EI structure [EI(ΔHD)] causes the loss of HPr binding (see Table 2 and Figure 4).

Differential scanning calorimetry experiments (*17*, *18*, *31*) indicate that the N-terminal domain of EI is less stable than EIN itself. This suggests that an interaction between EIC and EIN in intact EI results in a conformational change, perhaps in HD. This conformational change may explain the previously observed specificity for interaction with HPr characteristic of intact EI (*22*), which is compromised in EIN.

Although it was not possible to demonstrate by ITC an association of HD with EI(ΔHD), reconstitution experiments established a transient association between these two fragments. Using [^{32}P]PEP, EI(ΔHD) can participate in phosphoryl transfer via HD to HPr. A quantitative analysis of the reconstitution, measuring phosphorylation of [^{14}C]methyl α-glucoside, demonstrated that the reconstituted activity is approximately 1000 times less than that with EI. It is apparent that the spatial arrangement of HD with respect to the active-site histidine of intact EI substantially promotes the phosphotransfer to HPr.

Reconstitution of PTS activity has also been successfully accomplished with mixtures of EIN and EIC from *M. capricolum* (Figure 7, inset to panel A). A similar reconstitution using fragments from *E. coli* (*33*) has been reported. It appears that the efficacy of reconstitution, reported here, by HD and EI(ΔHD) is substantially greater (at least 20 times) than that observed for the EIN−EIC pair. Whether this reflects a difference in the capability of the various fragments to interact with each other or some other features remains to be established.

Fomenkov et al. (*33*) reported that attempts to express isolated *E. coli* EIC were unsuccessful and concluded that EIC is unstable and rapidly proteolyzed in vivo. They were able to isolate EIC in vitro from a fusion protein construct. It is instructive to review our experiences with attempts to express *M. capricolum* EIC. A construct encoding M(His)$_6$M-(213−end) was not expressed. However, a somewhat shorter construct encoding M(His)$_6$M(249−end) (see Table 1) was expressed as well as was the EIN construct M(His)$_6$(1−268). Therefore, it is quite likely that preparations of *E. coli* EIC could be made providing a construct encoding the appropriate length of product was used.

Purified preparations of *M. capricolum* EI(ΔHD) have been crystallized (O. Herzberg, personal communication). The elucidation of the crystal structure, now underway, will be a valuable addition to these studies. Furthermore, the structure of EI(ΔHD), in conjunction with the structure of EIN (*5*, *6*) will allow for a prediction of the complete three-dimensional structure of EI.

In summary, these studies have unequivocally established the importance of the helical subdomain of the amino-terminal domain of EI for the interaction with HPr. The covalent linkage of HD to EI(ΔHD) accomplishes an increase in the phosphotransfer potential of approximatley 1000-fold. This probably explains the evolution of the tethering of HD to EI(ΔHD) resulting in the multifunctional EI.

ACKNOWLEDGMENT

The authors are grateful to Dr. James Gruschus for his help in rendering the model for EI structure. *E. coli* EI and IIA^{glc} were gifts from Dr. Yeong-Jae Seok and *E. coli* HPr was kindly provided by Dr. Melissa Sondej. We thank Dr. Osnat Herzberg for helpful discussions and for a critical review of the manuscript.

REFERENCES

1. Postma, P. W., Lengeler, J. W., and Jacobson, G. R. (1996) in *Escherichia coli* and Salmonella: Cellular and Molecular Biology (Neidhardt, F. C., Ed.) pp 1149−1174, ASM Press, Washington DC.
2. Herzberg, O., and Klevit, R. (1994) *Curr. Opin. Struct. Biol. 4*, 814−822.
3. Huang, K., Kapadia, G., Zhu, P.-P., Peterkofsky, A., and Herzberg, O. (1998) *Structure 6*, 697−710.
4. Pieper, U., Kapadia, G., Zhu, P.-P., Peterkofsky, A., and Herzberg, O. (1995) *Structure 3*, 781−790.
5. Liao, D.-I., Silverton, E., Seok, Y.-J., Lee, B. R., Peterkofsky, A., and Davies, D. R. (1996) *Structure 4*, 861−872.
6. Garrett, D. S., Seok, Y.-J., Liao, D.-I., Peterkofsky, A., Gronenborn, A. M., and Clore, G. M. (1997) *Biochemistry 36*, 2517−2530.
7. Goss, N. H., Evans, C. T., and Wood, H. G. (1980) *Biochemistry 19*, 5805−5809.
8. Carroll, L. J., Xu, Y., Thrall, S. H., Martin, B., and Dunaway-Mariano, D. (1994) *Biochemistry 33*, 1134−1142.
9. Pocalyko, D. J., Carroll, L. J., Martin, B. M., Babbitt, P. C., and Dunaway-Mariano, D. (1990) *Biochemistry 29*, 10757−10765.
10. Herzberg, O., Chen, C. C., Kapadia, G., McGuire, M., Carroll, L. J., Noh, S. J., and Dunaway-Mariano, D. (1996) *Proc. Natl. Acad. Sci. U.S.A. 93*, 2652−2657.
11. Garrett, D., Seok, Y.-J., Peterkofsky, A., Clore, G. M., and Gronenborn, A. M. (1997) *Biochemistry 36*, 4393−4398.
12. Garrett, D. S., Seok, Y.-J., Peterkofsky, A., Gronenborn, A. M., and Clore, G. M. (1999) *Nat. Struct. Biol. 6*, 166−173.
13. Zhu, P.-P., Reizer, J., Reizer, A., and Peterkofsky, A. (1993) *J. Biol. Chem. 268*, 26531−26540.
14. Zhu, P.-P., Reizer, J., and Peterkofsky, A. (1994) *Protein Sci. 3*, 2115−2128.
15. Zhu, P.-P., Lecchi, P., Pannell, L., Jaffe, H., and Peterkofsky, A. (1995) *Protein Expression Purif. 6*, 189−195.
16. Zhu, P.-P., Nosworthy, N., Ginsburg, A., Miyata, M., Seok, Y.-J., and Peterkofsky, A. (1997) *Biochemistry 36*, 6947−6953.
17. Nosworthy, N. J., Peterkofsky, A., König, S., Seok, Y.-J., Szczepanowski, R. H., and Ginsburg, A. (1998) *Biochemistry 37*, 6718−6726.
18. Chauvin, F., Fomenkov, A., Johnson, C. R., and Roseman, S. (1996) *Proc. Natl. Acad. Sci. U.S.A. 93*, 7028−7031.
19. Reddy, P., Fredd-Kuldell, N., Liberman, E., and Peterkofsky, A. (1991) *Protein Expression Purif. 2*, 179−187.
20. Zhu, P.-P., Herzberg, O., and Peterkofsky, A. (1998) *Biochemistry 37*, 11762−11770.
21. Sanger, F., Nicklen, S., and Coulson, A. R. (1977) *Proc. Natl. Acad. Sci. U.S.A. 74*, 5463−5467.

22. Seok, Y.-J., Lee, B. R., Zhu, P.-P., and Peterkofsky, A. (1996) *Proc. Natl. Acad. Sci. U.S.A. 93*, 347−351.
23. Waddell, W. J. (1956) *J. Lab. Clin. Med. 48*, 311−314.
24. Zamyatnin, A. (1984) *Annu. Rev. Biophys. Bioeng. 13*, 145−165.
25. Yang, J. T., Wu, C. S., and Martinez, H. M. (1986) *Methods Enzymol. 130*, 208.
26. Levy, S., Zeng, G.-Q., and Danchin, A. (1990) *Gene 86*, 27−33.
27. Seok, Y.-J., Zhu, P.-P., Koo, B.-M., and Peterkofsky, A. (1999) *Biochem. Biophys. Res. Commun. 250*, 381−384.
28. Chauvin, F., Fomenkov, A., Johnson, C. R., and Roseman, S. (1996) *Proc. Natl. Acad. Sci. U.S.A. 93*, 7028−7031.
29. Chauvin, F., Brand, L., and Roseman, S. (1996) *Res. Microbiol. 147*, 471−479.
30. Waygood, E. B. and Steeves, T. (1980) *Can. J. Biochem. 58*, 40−48.
31. LiCalsi, C., Crocenzi, T. S., Freire, E., and Roseman, S. (1991) *J. Biol. Chem. 266*, 19519−19527.
32. Lee, B. R., Lecchi, P., Pannell, L., Jaffe, H., and Peterkofsky, A. (1994) *Arch. Biochem. Biophys. 312*, 121−124.
33. Fomenkov, A., Valiakhmetov, A., Brand, L., and Roseman, S. (1998) *Proc. Natl. Acad. Sci. U.S.A. 95*, 8491−8495.

BI991680P